AGU Advances

Key Points:

- We used clean-access hot water drilling to sample water and sediment from an active subglacial lake in West Antarctica
- The presence of natural-level radiocarbon in sediment and water samples enabled us to trace the subglacial carbon cycle
- We find that the deglacial extent of grounding line retreat reached up to 250 km inland of present before re-advancing in the Holocene

Correspondence to:

R. A. Venturelli and B. E. Rosenheim,
Venturelli@mines.edu;
Brosenheim@usf.edu

Constraints on the Timing and Extent of Deglacial Grounding Line Retreat in West Antarctica

Ryan A. Venturelli[1] , Brenna Boehman[2] , Christina Davis[3], Jon R. Hawkings[4] , Sarah E. Johnston[5], Chloe D. Gustafson[6] , Alexander B. Michaud[7] , Cyrille Mosbeux[6], Matthew R. Siegfried[1] , Trista J. Vick-Majors[8] , Valier Galy[2], Robert G. M. Spencer[9] , Sophie Warny[10], Brent C. Christner[3], Helen A. Fricker[6], David M. Harwood[11] , Amy Leventer[12] , John C. Priscu[13] , Brad E. Rosenheim[14] , and SALSA Science Team

[1]Colorado School of Mines, Golden, CO, USA, [2]Woods Hole Oceanographic Institution, Woods Hole, MA, USA, [3]University of Florida, Gainesville, FL, USA, [4]University of Pennsylvania, Philadelphia, PA, USA, [5]University of Alaska Fairbanks, Fairbanks, AK, USA, [6]Scripps Institution of Oceanography, La Jolla, CA, USA, [7]Bigelow Laboratory for Ocean Sciences, East Boothbay, ME, USA, [8]Michigan Technological University, Houghton, MI, USA, [9]Florida State University, Tallahassee, FL, USA, [10]Louisiana State University, Baton Rouge, LA, USA, [11]University of Nebraska-Lincoln, Lincoln, NE, USA, [12]Colgate University, Hamilton, NY, USA, [13]Polar Oceans Research Group, Sheridan, MT, USA, [14]College of Marine Science, University of South Florida, St. Petersburg, FL, USA

Abstract Projections of Antarctica's contribution to future sea level rise are associated with significant uncertainty, in part because the observational record is too short to capture long-term processes necessary to estimate ice mass changes over societally relevant timescales. Records of grounding line retreat from the geologic past offer an opportunity to extend our observations of these processes beyond the modern record and to gain a more comprehensive understanding of ice-sheet change. Here, we present constraints on the timing and inland extent of deglacial grounding line retreat in the southern Ross Sea, Antarctica, obtained via direct sampling of a subglacial lake located 150 km inland from the modern grounding line and beneath >1 km of ice. Isotopic measurements of water and sediment from the lake enabled us to evaluate how the subglacial microbial community accessed radiocarbon-bearing organic carbon for energy, as well as where it transferred carbon metabolically. Using radiocarbon as a natural tracer, we found that sedimentary organic carbon was microbially translocated to dissolved carbon pools in the subglacial hydrologic system during the 4.5-year period of water accumulation prior to our sampling. This finding indicates that the grounding line along the Siple Coast of West Antarctica retreated more than 250 km inland during the mid-Holocene (6.3 ± 1.0 ka), prior to re-advancing to its modern position.

Plain Language Summary Our continuous observations of the Antarctic Ice Sheet cover only the last three decades, so we must employ the geologic record to contextualize our ongoing observations and improve models that predict Antarctica's future contributions to sea level rise. In this study, we melted through over 1 km of ice to collect sediment and water from a freshwater lake at the base of the West Antarctic Ice Sheet. We found that this region, now 150 km from the modern ocean, was part of the marine environment only a few thousand years ago. That past connection to the ocean is powering today's population of microbial life, which moves carbon from the sediment to the water column in the lake and is eventually flushed into the Southern Ocean. We calculated the rates of carbon transfer and found that ice retreat following the Last Glacial Maximum did not stop at our study site but must have extended much farther inland. Our work highlights that we have not yet sampled the maximum extent of the last deglaciation. Investigating the conditions that enabled Antarctic ice to re-advance from this far inland position may help inform us about how the ice sheet may be able to recover from the ongoing ice mass loss.

1. Introduction

The Antarctic Ice Sheet (AIS) has been losing mass over the past few decades because of ice dynamic processes (Rignot et al., 2019; Smith et al., 2020) with the potential to trigger amplifying feedbacks in marine sectors (e.g., Mercer, 1978; Schoof, 2007; Weertman, 1974). However, our modern continuous observational record remains too short to fully quantify processes governing mass loss or their full effect on coastal populations (Meredith et al., 2019; Nicholls et al., 2021). As a result, uncertainty of our projections is dominated by the unknown

Formal analysis: Ryan A. Venturelli, Brenna Boehman, Christina Davis, Jon R. Hawkings, Alexander B. Michaud, Cyrille Mosbeux, Matthew R. Siegfried, Trista J. Vick-Majors, Sophie Warny, David M. Harwood, Amy Leventer, Brad E. Rosenheim

Funding acquisition: Ryan A. Venturelli, Jon R. Hawkings, Brent C. Christner, Helen A. Fricker, Amy Leventer, John C. Priscu, Brad E. Rosenheim

Investigation: Ryan A. Venturelli, Christina Davis, Chloe D. Gustafson, Alexander B. Michaud, Matthew R. Siegfried, Trista J. Vick-Majors, Brent C. Christner, Helen A. Fricker, David M. Harwood, Amy Leventer, John C. Priscu, Brad E. Rosenheim

Methodology: Ryan A. Venturelli, Brenna Boehman, Christina Davis, Jon R. Hawkings, Alexander B. Michaud, Cyrille Mosbeux, Matthew R. Siegfried, Trista J. Vick-Majors, Sophie Warny, David M. Harwood, Amy Leventer, Brad E. Rosenheim

Project Administration: Ryan A. Venturelli, John C. Priscu, Brad E. Rosenheim

Resources: Ryan A. Venturelli, Brenna Boehman, Jon R. Hawkings, Valier Galy, Sophie Warny

Supervision: Valier Galy, Robert G. M. Spencer, Brent C. Christner, Helen A. Fricker, John C. Priscu, Brad E. Rosenheim

Visualization: Ryan A. Venturelli, Matthew R. Siegfried, Sophie Warny, Amy Leventer, Brad E. Rosenheim

Writing – original draft: Ryan A. Venturelli, Matthew R. Siegfried, Brent C. Christner, Helen A. Fricker, Brad E. Rosenheim

Writing – review & editing: Ryan A. Venturelli, Brenna Boehman, Christina Davis, Jon R. Hawkings, Sarah E. Johnston, Chloe D. Gustafson, Alexander B. Michaud, Cyrille Mosbeux, Matthew R. Siegfried, Trista J. Vick-Majors, Valier Galy, Robert G. M. Spencer, Sophie Warny, Brent C. Christner, Helen A. Fricker, David M. Harwood, Amy Leventer, John C. Priscu, Brad E. Rosenheim

strength of marine ice-sheet feedbacks and internal climate variability (Robel et al., 2019). Records of ice-sheet change in the geologic past (i.e., paleoglaciological reconstructions) provide a pathway for constraining the limits of ice-mass changes over societally relevant timescales (Jones et al., 2022; Kopp et al., 2016), and as a result, may reduce the uncertainty envelope in projections of future sea level rise (e.g., DeConto et al., 2021).

Conventionally, we have reconstructed deglaciation from the Last Glacial Maximum (LGM) with a combination of: (a) cosmogenic nuclide exposure dating of bedrock and glacially transported erratics above the modern ice surface and near glacier termini to provide constraints on past thinning (e.g., Stone et al., 2003); and (b) a combination of geomorphic data and sediment cores obtained from outboard of modern ice margins to provide constraints on the style and timing of past retreat (e.g., Prothro et al., 2018, 2020). These methods enable us to reconstruct when ice retreated from a location; however, they likely do not provide a full picture of more complicated ice histories (e.g., Greenwood et al., 2018). Emerging evidence from model simulations (Kingslake et al., 2018), paleoglaciological reconstructions (Venturelli et al., 2020), gaps in the above-ice glacial-geologic record (Johnson et al., 2022), and modern observations (King et al., 2022) indicates that grounding lines around Antarctica likely retreated inland of present during deglaciation from the LGM and have recently readvanced to the configuration we observe today. Such a retreat scenario implies that we do not yet know the southernmost extent of deglacial grounding line retreat; therefore, we cannot fully assess the sensitivity of AIS to past drivers of this most recent deglaciation or quantify the internal and external mechanisms that enabled readvance. Identifying the timing and extent of inland grounding line retreat requires access to geologic archives beneath modern ice cover (Johnson et al., 2022) which is limited due to logistical challenges of sampling the subglacial environment (NRC, 2007).

The few opportunities we have had to drill through AIS and recover sediments at its base have revealed that subglacial sediments in some parts of West Antarctica contain radiocarbon (^{14}C) (Kingslake et al., 2018; Venturelli et al., 2020). Because the modern subglacial environment in Antarctica is sealed by an ice sheet that inhibits contemporary exchange of atmospheric or marine (i.e., ^{14}C-bearing) CO_2, the existence of ^{14}C in subglacial carbon reservoirs indicates a past connection between the presently isolated subglacial environment and the atmospherically connected marine environment within the last 50 kyr. Antarctica's grounding lines separate marine from subglacial environments as they mark the transition from grounded ice sheet to floating ice shelf. When the grounding line retreats, the grounded area of AIS decreases, and sediments that were previously subglacial become exposed to sub-ice-shelf conditions. This process introduces seawater, enabling production of fresh, ^{14}C-bearing organic matter through dark carbon fixation metabolisms. When the grounding line re-advances, ^{14}C-bearing organic matter becomes preserved in the subglacial sedimentary record together with previously deposited (^{14}C-free) sediments. Thus far, subglacial ^{14}C has been used to infer where (Kingslake et al., 2018) and determine when (Venturelli et al., 2020) AIS grounding lines retreated inboard of present during the last deglaciation, but how ^{14}C-bearing carbon is incorporated in the subglacial sedimentary environment remains unknown.

It has been suggested that the 650 subglacial lakes present beneath AIS may contain understudied and valuable sediment archives of ice-sheet history (Bentley et al., 2011; Livingstone et al., 2022; Siegfried et al., 2023; Yan et al., 2022). Use of ^{14}C from these subglacial lake sediment archives as a chronometer of Holocene grounding line retreat requires a full understanding of the source and cycling of carbon in the subglacial aquatic environment. This is because knowledge of carbon incorporation pathways is imperative for determining the form of carbon present, which impacts the validity of radiocarbon results (Libby, 1955). In this study, we sampled sediment and water from a subglacial lake beneath the West Antarctic Ice Sheet (WAIS) to answer (a) when the grounding line retreated inland of present during the last deglaciation (i.e., the timing of ^{14}C input), and (b) how ^{14}C deposited during this latest marine incursion is cycled through the subglacial hydrologic system. With a combination of thermal decomposition and compound specific isotope analysis (CSIA) of acid insoluble organic matter (AIOM) from these sediments, we determined that the grounding line retreated over our study site and caused a marine incursion, filling the catchment with marine water 6.3 ± 1.0 ka, during the mid-Holocene. With knowledge of the precise timing of marine incursion to this area and inputs to the contemporary lake environment, we used ^{14}C measured in dissolved carbon reservoirs to assess microbial translocation of ^{14}C from sediment to water within the subglacial environment. By combining these new data with measurements of contemporary microbial metabolism, we conclude that the southernmost limit of grounding line retreat may have been more than 250 km inboard of present during the last deglaciation. Our results highlight that we have not yet sampled the inland extent of the last deglaciation in West Antarctica, and further subglacial drilling efforts will be required to do so.
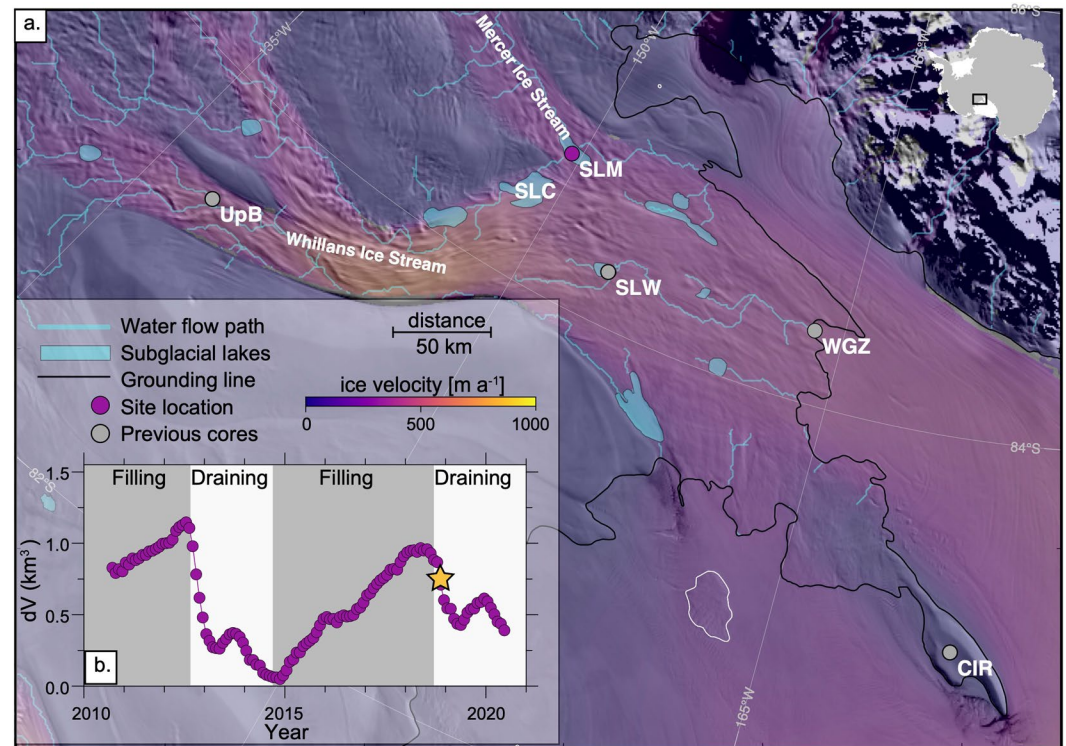
Figure 1. (a) Southern Ross Sea sector ice streams with previous subglacial core locations (Whillans Subglacial Lake (SLW; Tulaczyk et al., 2014), Whillans Grounding Zone (WGZ; Venturelli et al., 2020), the upstream site at of Whillans Ice Stream (UpB; Engelhardt & Kamb, 1997), and Crary Ice Rise (CIR; Bindschadler et al., 1988) marked with gray circles, Mercer Subglacial Lake (SLM) indicated with a purple circle, and the lake directly upstream Conway Subglacial Lake (SLC) labeled. Ice velocity (Mouginot et al., 2019) is overlain on an imagery mosaic (Scambos et al., 2007), with active subglacial lake areas (blue polygons; Siegfried & Fricker, 2018), hydropotential flow paths (blue lines; Siegfried & Fricker, 2018), and grounding line (black; Depoorter et al., 2013) indicated. (b) Volume changes in Mercer Subglacial Lake inferred from CryoSat-2 radar altimetry (Siegfried et al., 2023) with a yellow star marking the timing of sampling.

2. Materials and Methods

2.1. Site Description and Sample Collection

During the 2018–2019 austral summer, the Subglacial Antarctic Lakes Scientific Access (SALSA) Science Team used a clean-access (Michaud et al., 2020; Priscu et al., 2013), hot-water drill (Priscu et al., 2021; Rack, 2016) to melt a 0.4 m diameter borehole through 1,087 m of ice at the confluence of Whillans and Mercer ice streams to access an active subglacial lake (Figure 1). Mercer Subglacial Lake is a freshwater lake sourced entirely by basal melt of the overlying AIS—with a portion of its water sourced from the base of the East Antarctic Ice Sheet (EAIS) (Carter & Fricker, 2012) and a portion of its water from the drainage of Conway Subglacial Lake immediately upstream beneath WAIS (Siegfried et al., 2016). Once full, Mercer Subglacial Lake releases water to downstream lakes and eventually across the grounding line into the Ross Sea (Carter et al., 2013). Nearly two decades of satellite altimetry data illustrate that Mercer Subglacial Lake completes a fill-drain cycle every four to 6 years (Siegfried & Fricker, 2018; Siegfried et al., 2023), and at the time of sampling had just entered its draining phase after accumulating water for 4.5 years (Figure 1b).

The water column was 15 m deep at the time of access, and over the 8.6 days of scientific operations, we collected 60 L of lake water from the middle (7.5 m depth) of the water column (Priscu et al., 2021). We deployed a Uwitec multicoring device to retrieve 10 multicores (0.32–0.49 m) and a newly developed borehole gravity coring device to retrieve two free fall (gravity) cores (1.0 and 1.76 m) (Rosenheim et al., 2023). Our field operations followed a strict ^{14}C-clean protocol (detailed in Venturelli et al., 2021) to separate discrete aliquots of lake water for isotopic analysis. We decanted water collected for isotopic analysis of dissolved organic carbon (DOC) from a clean Niskin bottle into a pre-combusted (525°C; 4 hr) 1 L amber glass bottle and immediately froze the samples. We decanted

Table 1
Sample Intervals for Each Mercer Subglacial Lake Sediment Core Used for Geochemical Analysis

Core name	Core type	Core length (cm)	EA-IRMS sample interval	RPO ^{14}C sample interval
01UW-A	Multicore	49	Top and bottom of each lithologic unit	4–6 cm, 16–18 cm, 44–46 cm
01UW-C	Multicore	44	Every 2 cm	None
01FF	Gravity core	100	Every 4 cm	45–50 cm, 57–58 cm, 65–66 cm, 73–74 cm, 80–85 cm
02FF	Gravity core	176	Top and bottom of each lithologic unit	5–7 cm, 148-50 cm, 168–170 cm

Note. We sampled evenly throughout the 2.06 m composite section for EA-IRMS analyses and focused sampling the boundaries of each lithologic unit for RPO ^{14}C.

water collected for isotopic analysis of dissolved inorganic carbon (DIC) into pre-combusted (525°C; 4 hr) 500 mL glass bottle pre-loaded with 20 μL of a saturated HgCl$_2$ solution. We shipped all water samples directly from the field to the National Ocean Sciences Accelerator Mass Spectrometry (NOSAMS) Facility. Sediment cores included in this study were capped immediately upon recovery from the borehole and stored upright during shipment and storage at 4°C. We wrapped two cores from the first multicore cast (01UW-A and 01UW-C) and two free fall cores (01FF and 02FF) intended for isotopic analyses with multiple layers of plastic wrapping for shipment to the Oregon State University Marine and Geology Repository (OSU-MGR) to avoid any contamination in the field, during packaging, and through shipment (see Venturelli et al., 2021). Similarities in magnetic susceptibility and lithology allowed for the construction of a continuous 2.06 m composite section representing the transition from sub-ice stream deposition at depth to lake deposition in core tops (Figure S1 in Supporting Information S1).

2.2. Isotopic Analyses of Subglacial Lake Water

At NOSAMS, we filtered (Pall Life Sciences, 2.5 cm diameter, PALL number 7200) 1 L of subglacial lake water prior to preparation for isotopic analyses (δ^{13}C; Δ^{14}C) of DOC. We acidified (1N HCl), rinsed (deionized water), and dried the filtered residue to isotopically characterize particulate organic carbon (POC) in the Mercer Subglacial Lake water column. Once dry, we packed the entire filter into a pre-combusted (900°C, 4 hr) quartz ampoule with copper oxide and silver wire, combusted the closed ampoule (900°C, 4 hr), and cryogenically purified the CO$_2$ evolved from POC. To prepare the filtered 1 L water sample for isotopic analyses of DOC, we followed the methods of Xu et al. (2021). To prepare samples for isotopic analyses of DIC, we followed the methods described in McNichol et al. (1994). We converted all CO$_2$ samples evolved from POC, DOC, and DIC sample preparations to graphite by reduction on an iron catalyst using the closed-tube, zinc catalyst method (Walker & Xu, 2019) before determination of ^{14}C/^{12}C ratios and δ^{13}C at NOSAMS.

2.3. Isotopic Analyses of Subglacial Lake Sediment

2.3.1. Bulk Sediment Geochemistry

Multicores 01UW-A and 01UW-C consist of two lithologic units, with 12 cm of laminated mud interpreted as deposition within the modern Mercer Subglacial Lake setting (Siegfried et al., 2023) underlain by a massive clast-rich muddy diamict unit, interpreted as sub-ice-stream sedimentation (e.g., Kamb, 2001), that persists also in gravity cores 01FF and 02FF (Figure S1 in Supporting Information S1). We removed 1–3 g (wet) samples for analysis with EA-IRMS to have even sample coverage throughout the 2.06 m composite section and 5–10 g (wet) samples for ramped pyrolysis and oxidation (Ramped PyrOx or RPO) to measure ^{14}C at the top and bottom of depositional units (Table 1).

We dried, homogenized, and acid rinsed each sample with 1N HCl to remove carbonate minerals. Following decarbonation, we removed residual acid with a series of deionized water rinses until the supernatant asymptotically approached a pH near neutrality (pH = 6–7). Remaining AIOM was dried and stored in pre-combusted (525°C; 4 hr) glass scintillation vials until analysis. During the first round of decarbonation of these samples, we noticed effervescence substantial enough, if CO$_2$, to be conducive to isotope analysis. We thus reserved a subset of samples (N = 6) to remain untreated for analysis of the carbonate mineral component.

We determined total organic carbon (% TOC) and bulk stable isotope composition (δ^{13}C) for all AIOM samples with a Carlo-Erba NAN2500 Series-II Elemental Analyzer coupled to a continuous-flow Thermo-Finnigan Delta + XL IRMS. We used NIST 8573 and NIST 8574 as calibration standards and a low carbon, bulk Antarctic sediment sample

(JGC20C) as a working standard. Analytical uncertainty, expressed as ± 1 standard deviation of replicate measurements of the working standard, was $\pm 0.02\%$ for %TOC and 0.5‰ for $\delta^{13}C$ during our analysis period. For analyses of the carbonate mineral component, we hydrolyzed the subset ($N = 6$) of sediment samples that had not been decarbonated with 85% phosphoric acid (H_3PO_4) under vacuum at NOSAMS. We cryogenically purified and flame sealed into pre-combusted (525°C; 4 hr) borosilicate ampoules all CO_2 evolved from hydrolysis of carbonate minerals.

2.3.2. Ramped PyrOx ^{14}C

We applied RPO to separate the small amount of ^{14}C-bearing organic carbon from the abundance of pre-aged organic carbon in AIOM samples from this subglacial mixture. Using RPO, we separated pyrolysates into three discrete CO_2 aliquots for each sediment depth. We based sampling on the shape of thermographs (i.e., CO_2 evolved with temperature) in the RPO process (Figure S2 in Supporting Information S1), sampling the first aliquot of CO_2 at the top of the first peak on each thermograph (~400°C), the second at the completion of the first peak (~700°C), and the third at the completion of the pyrolysis reaction (at 1,000°C) following the methods of Rosenheim et al. (2008).

Subt et al. (2017) demonstrated that minimizing the size of low temperature RPO aliquots can limit the bias of pre-aged, allochthonous carbon in Antarctic margin sediments. To approach a maximum radiocarbon concentration present in Mercer Subglacial Lake sediments, we also applied a modified RPO method, wherein we repeatedly combusted four 400 mg sediment samples from the same depth from a sampled interval to collect ultra-small (8 μmol each), low-temperature aliquots (collected at ~270°C; Figure S2 in Supporting Information S1). We combined these low temperature CO_2 aliquots for isotopic analysis as a single sample following the composite RPO technique described in Subt et al. (2017). Samples dated with the composite RPO technique are referred to hereafter a "combo" aliquots. All CO_2 aliquots produced with the preparatory techniques described above (RPO and carbonate hydrolysis) were analyzed at NOSAMS for $^{14}C/^{12}C$ ratios and $\delta^{13}C$. We blank-corrected all RPO data following the methods described in Fernandez et al. (2014) with updated blank masses detailed in Venturelli et al. (2020).

2.3.3. Compound Specific Isotope Analysis

In addition to RPO of organic matter for isotopic analyses, we also performed chemical separation of a subset of sediment aliquots from one core (01FF). We extracted freeze dried samples (~1 g from 45 to 50 cm and 80–85 cm) at 100°C for 20 min in a microwave accelerated reaction system in 15 mL of dichloromethane (DCM) and methanol (9:1). We trimethylsilyl derivatized an aliquot of the total lipid extract (TLE) and screened it for chemical compounds present using: (a) a Hewlett Packard 5890 gas chromatography-flame ionization detector (GC-FID) with a Gerstel PTV injection system and separated with a VF-1MS capillary column; and (b) a Thermo Scientific Trace 1310 GC analyzer coupled to an Thermo Scientific ISQ single quadrupole mass spectrometer with an AI 1310 injection system and separated with a TG- 5MS capillary column. We separated TLE by column chromatography using 1 g of Supelclean amino-propyl silica gel (Supelco Analytical) using the following elution scheme: 4 mL hexane (F1); 7 mL hexane and DCM (4:1, F2); 10 mL DCM and acetone (9:1, F3); 14 mL 2% (w/w) formic acid in DCM (F4); 18 mL DCM and methanol (1:1, F5). For analysis of n-alkanoic acids, F4 was methylated with acidified methanol of known isotopic composition and further separated by column chromatography (French et al., 2018). We analyzed fractions on GC-FID, GC-MS and HPLC-MS (Agilent 1200 series high-pressure liquid chromatography coupled to an Agilent LC/MSD SL quadrupole MS), as initially described by Hopmans et al. (2016) to examine the chemical compounds present.

We determined the $\delta^{13}C$ values of butyl esters and methylated n-alkanoic acids using GC-IRMS at Woods Hole Oceanographic Institution. We performed this analysis using a Hewlett Packard 6890 with a DB-1MS capillary column coupled to a Thermo Delta V IRMS via a GC/C combustion interface modified for oxygen trickle flow (Sessions, 2006). We measured all samples in triplicate, with the exception of C32 and C34 FAMES which were sample-limited, and calibrated against pulses of CO_2 gas with a known $\delta^{13}C$ value. Data are reported relative to Pee-Dee Belemnite. Unfortunately, we did not have enough butyl esters or methylated n-alkanoic acids for ^{14}C measurements.

2.4. Microbial Respiration

To assess movement of carbon from Mercer Subglacial Lake sediments to DIC in the water column, we determined rates of microbial respiration at the sediment-water interface following methods described by Vick-Majors et al. (2016). Briefly, we amended duplicate water samples (5 ml) and one killed (250 μl of cold trichloroacetic

Table 2
Mercer Subglacial Lake Carbon Reservoirs and Results From Carbon Concentration Measurements, Carbon Stock Assessment, and Radiocarbon Analysis

Reservoir	Reservoir size[a]	Carbon concentration	Carbon stock[b, c]	Radiocarbon concentration ($\Delta^{14}C$)
Water column DOC	7.15×10^{11} L	5.1×10^{-5} mol L^{-1}	4.38×10^{8} g C	−947‰
Water column DIC	7.15×10^{11} L	8.96×10^{-4} mol L^{-1}	7.69×10^{9} g C	−979‰
Water column POC	7.15×10^{11} L	0.4% TOC	5.72×10^{9} g C	−923‰
Sediment OC[d]	2.94×10^{14} cm^3	0.15% TOC	8.69×10^{11} g C	−792‰

[a]Lake volume was determined using an average depth of 5 m inferred by area-averaged height anomaly (Siegfried & Fricker, 2018) and the published lake area of 143 km^2 (Siegfried & Fricker, 2021). [b]Carbon stocks in the water column were determined by multiplying carbon concentrations by the total lake volume of 7.15×10^{11} L described in footnote 1. [c]Carbon stocks in the sediment were determined by multiplying carbon concentrations by the full sediment depth (2.06 m) recovered from Mercer Subglacial Lake. [d]Geophysical measurements 30 km downstream show that sediments underlying Mercer and Whillans ice streams are 0.5–1.9 km thick (Gustafson et al., 2022). If this sediment package extends upstream to Mercer Subglacial Lake, carbon stock listed here should be regarded as a minimum carbon stock for SOC in this system.

acid; TCA) control with uniformly labeled ^{14}C-L-leucine (final concentration 60 nmol L^{-1}; final ^{14}C activity 0.018 μCi ml^{-1}) and incubated in autoclaved 25 ml glass side arm flasks. We sealed the flasks with butyl rubber septa equipped with a basket containing a folded glass fiber filter suspended above the aqueous phase as a CO_2 trap. Following incubation in the dark for 72 hr at 2–4°C, we terminated incubations by the addition of cold 100% TCA, lowering the pH to ∼2. We added ß-phenylethylamine (100 μL; Sigma) to the glass fiber filter to trap respired CO_2 from the headspace gas. We incubated killed and acidified samples at ∼25°C for 24 hr with occasional gentle swirling to ensure the release of CO_2 from the aqueous phase. We then removed the glass fiber filters from the basket, placed in 10 ml glass scintillation vials, and, following the addition of 10 ml of Cytoscint-ES$^{\text{tm}}$ scintillation cocktail, determined ^{14}C activity on a calibrated scintillation counter. We converted ^{14}C-leucine respiration to units of carbon using the following conversion factors: 1.4×10^{17} cells mol^{-1} leucine (Chin-Leo & Kirchman, 1988) and 11 fg C cell^{-1} (Kepner et al., 1998). We used respiration rates measured at the sediment-water interface to assess the translocation of ^{14}C from sediments to the water column.

3. Results

3.1. Subglacial Lake Carbon Stock

We found that sediments are the dominant carbon reservoir in Mercer Subglacial Lake, with several orders of magnitude more carbon than each of the water column carbon reservoirs (DIC, DOC, and POC; Table 2). The sedimentary organic carbon (SOC) in Mercer Subglacial Lake contained ^{14}C throughout the entire recovered sediment column, similar to previous work in this region (Kingslake et al., 2018; Venturelli et al., 2020); however, our new results show that SOC contained more ^{14}C than any other reservoir in the subglacial system. The DOC reservoir contained a higher ^{14}C concentration than what was present in the DIC reservoir. In the water column, POC contained more ^{14}C than either of the reservoirs of dissolved carbon (i.e., DIC, DOC). Carbon concentrations and bulk isotopic composition of water column POC mirrored those of SOC, implying a similar source.

3.2. Age and Source of Organic Matter in Subglacial Lake Sediments

In addition to the presence of ^{14}C in Mercer Subglacial Lake sediments (Table 2), other chronologic constraints indicated discrete intervals of marine sedimentation across the West Antarctic basin. Recovered sediments contain a wide range of time-diagnostic microfossils and source specific biomarkers deposited in both marine (diatoms, silicoflagellates, ebridians, sponge spicules, chrysophycean cysts) and terrestrial (pollen, lignin phenols) environments (See Texts S1, S2, and S3 in Supporting Information S1). All microfossil age constraints predate the expansion of contemporary WAIS, with known biostratigraphic ranges indicating that they were eroded and transported from early Oligocene and late Miocene source strata upstream of Mercer Subglacial Lake (Text S2 in Supporting Information S1).

Lignin is more resistant to microbial degradation than other components of plant material and is therefore one of the most suitable preserved biomarkers of terrigenous input into aquatic environments (Hernes & Benner, 2006). Lignin phenol concentrations were very low in all core sediments sampled. The mean Σ6, lignin phenols only derived from terrestrial plant material (vanillyl and syringyl groups; Hernes et al., 2007), was 436 ± 299 ng gdw^{-1}
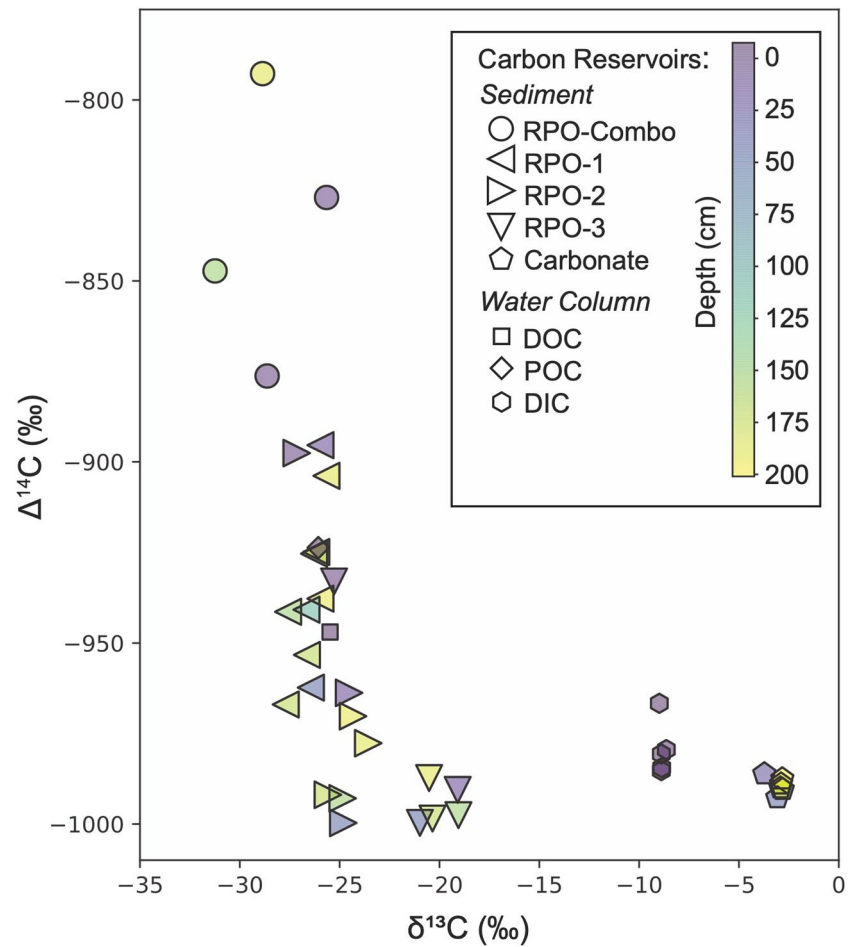
Figure 2. Distribution of isotopic data for all carbon reservoirs measured in Mercer Subglacial Lake. Here we demonstrate the spectrum of isotopic data in sediment samples prepared with RPO and distinct differences in $\delta^{13}C$ and $\Delta^{14}C$ values between inorganic and organic carbon reservoirs. A full description of RPO aliquots can be found in Section 2.3.2. All points are colored based on the depth from which they were collected in the lake where 0 represents the sediment-lake water interface and we note that we observed no relationship with depth (i.e., downcore trends) in either $\delta^{13}C$ or $\Delta^{14}C$ data. 2σ error bars are smaller than the size of individual data points.

(1SD), which is at the lowest end of literature values for sediments (North East Atlantic abyssal plain surficial sediment minimum ~400 ng gdw^{-1}; Gough et al., 1993). Carbon normalized lignin yields (λ_6) were 26 ± 13 µg 100 mg OC^{-1} (1SD). Comparable λ_6 values in the literature are from abyssal plain sediments far from continental inputs (24 ± 27 µg 100 mg OC^{-1}; Gough et al., 1993) where the predominant source of lignin is believe to be aeolian deposition of lignin-rich material on the ocean surface (Eglinton et al., 2002; Hernes & Benner, 2006), and continental shelf sediments that receive little terrestrial material and where marine-derived organic matter predominates the organic carbon pool (40–170 µg 100 mg OC^{-1}; Sun et al., 2017). Both the Σ_6 and λ_6 in Mercer Subglacial Lake sediments likely indicate little recent terrestrial influence in Antarctic subglacial lake systems and suggest extensive microbially driven degradation of lignin over long time periods. This hypothesis is supported by biostratigraphic ranges of terrestrial palynomorphs (Text S2, Figure S3 in Supporting Information S1).

Carbonate minerals throughout the entire sediment column were nearly devoid of ^{14}C with an average $\Delta^{14}C$ value of $-989‰$, decreasing by 1–2‰ every 10 cm downcore (Figure 2). In contrast, SOC throughout the recovered sediment column contained ^{14}C (Figure 2). We separated ^{14}C-bearing SOC from ^{14}C-free SOC with RPO. The highest directly measured $\Delta^{14}C$ values ($-792‰$), associated with the youngest age, were identified in diamict below the modern lake facies (Siegfried et al., 2023; Figure 2).

$\Delta^{14}C$ and $\delta^{13}C$ values for our RPO aliquots exhibited an inverse linear relationship, where lower $\delta^{13}C$ values corresponded to higher $\Delta^{14}C$ (Figures 2 and 3). Linear relationships such as this evolve from mixing between two end

members with distinct isotopic compositions; in the case of Mercer Subglacial Lake, the "old carbon" end member of this system is characterized by higher $\delta^{13}C$ values (-25 to $-20‰$) and no detectable ^{14}C ($\Delta^{14}C = -1000‰$), whereas the "new carbon" end member trends toward lower $\delta^{13}C$ values ($<-30‰$) and has a ^{14}C concentration that can be exploited to determine the timing of the latest marine incursion. If DIC from the Ross Sea ($2‰$; Villinski et al., 2000) were used for bacterial lipid production during this marine incursion (Achberger, 2016; Monson & Hayes, 1982), resultant organic matter could be characterized by a $\delta^{13}C$ as low as $-36‰$, meaning that our highest measured ^{14}C concentrations in SOC likely still reflect the incomplete separation of old carbon from new carbon incorporated during the most recent marine incursion (Rosenheim et al., 2008, 2013; Subt et al., 2017). Therefore, defining the most depleted $\delta^{13}C$ value in Mercer Subglacial Lake SOC is necessary to determine the $\Delta^{14}C$ value of the "new" endmember and, hence, the age of marine incursion. CSIA of lipids in the sediment display lower $\delta^{13}C$ values (n-alkanoic acid from fatty acids, minimum $\delta^{13}C = -33.9‰$) than low-temperature RPO aliquots (RPO-1 and RPO-combo; minimum $\delta^{13}C = -31.2‰$), suggesting CSIA provides a more useful $\delta^{13}C$ value for the "new" endmember. Using the most $\delta^{13}C$-depleted compound measured as our input, mean $\Delta^{14}C$ value for the "new" endmember by employing a Monte Carlo simulation to generate major axis regressions through 90% subsets of our data ($N = 32$) a total of 10,000 times. With this Monte Carlo simulation, we found the $\Delta^{14}C$ value associated with the new carbon endmember is $-566 \pm 25‰$ (Figure 3).

We found that the latest marine incursion reached Mercer Subglacial Lake during the mid-Holocene (6.3 ± 1.0 ka). This timing estimate reflects the median calibrated age and 2σ uncertainty as determined by the distribution of outcomes from our Monte Carlo simulation. To determine this result, we converted $\Delta^{14}C$ values to fraction modern and calculated the age (in ^{14}C years) of the latest marine incursion with a local reservoir correction of $1,101 \pm 120$ years following Venturelli et al. (2020). Finally, we calibrated this radiocarbon age (^{14}C years) to calendar age (yr B.P.) using Calib version 8.1 and the Marine20 data set (Heaton et al., 2020). We note that this estimate assumes biosynthetic isotope fractionation; the source of molecular compounds in subglacial sediments should be tested in future studies, for instance using compound specific radiocarbon analysis on dedicated sediment cores sampled specifically to have enough material for such detailed analysis.

4. Discussion

4.1. Assessing Source of the Young Carbon Endmember

Constraining the age of the new carbon endmember allows for quantification of the abundance of ^{14}C-bearing carbon in Mercer Subglacial Lake sediments, and along with $\delta^{13}C$, allows us to elucidate the source and abundance of ^{14}C in this subglacial environment. Using the $\Delta^{14}C$ value ($-566 \pm 25‰$) of the "new" end member in a two-component mixing model, we determined the amount of Holocene-aged carbon in the SOC reservoir to be 3.1% of the total 10^{11} g C SOC pool. Based on measurements of dark carbon fixation in the sub-ice-shelf environment (Horrigan, 1981; Priscu et al., 1990), this mass estimate is within realistic bounds of carbon fixation through chemolithoautotrophic production over the Mercer Subglacial Lake area during a short period (100s of years) of exposure to the marine environment. We interpret the finding of highly isotopically depleted lipids dominated by butyl esters to indicate high amounts of chemolithoautotrophic production at this site. When coupled with the size of the ^{14}C-bearing organic carbon reservoir, high proportions of butyl esters in the SOC support the interpretation that the new carbon endmember was produced by chemolithoautotrophic production of organic carbon in a sub-ice-shelf environment during the mid-Holocene (Venturelli et al., 2020), rather than metabolic waste from macrofauna which, despite being observed swimming in the sub-ice-shelf marine cavity (Kingslake et al., 2018; Neuhaus et al., 2021), left no trace in deposits at the base of Mercer Subglacial Lake.

4.2. Relating Microbial Metabolism to Grounding Line Retreat Extent

4.2.1. How Is Carbon Cycled in Mercer Subglacial Lake?

We used ^{14}C as a natural tracer of the subglacial carbon cycle in this low carbon environment, which is made possible by constraining the timing over which ^{14}C was sequestered in sediments (Figure 4). Our observation of the sediments being both the largest and youngest carbon reservoir indicates that subglacial sediments in contemporary Mercer Subglacial Lake provide the source of "fresh" carbon to the microbial ecosystem (Davis et al., 2023). Upstream sources of carbon dissolved in water and transported within subglacial sediments that fill Mercer Subglacial Lake should be devoid of ^{14}C as basal ice in this region dates to 68 ka (Buizert et al., 2015). Subglacial hydrologic modeling
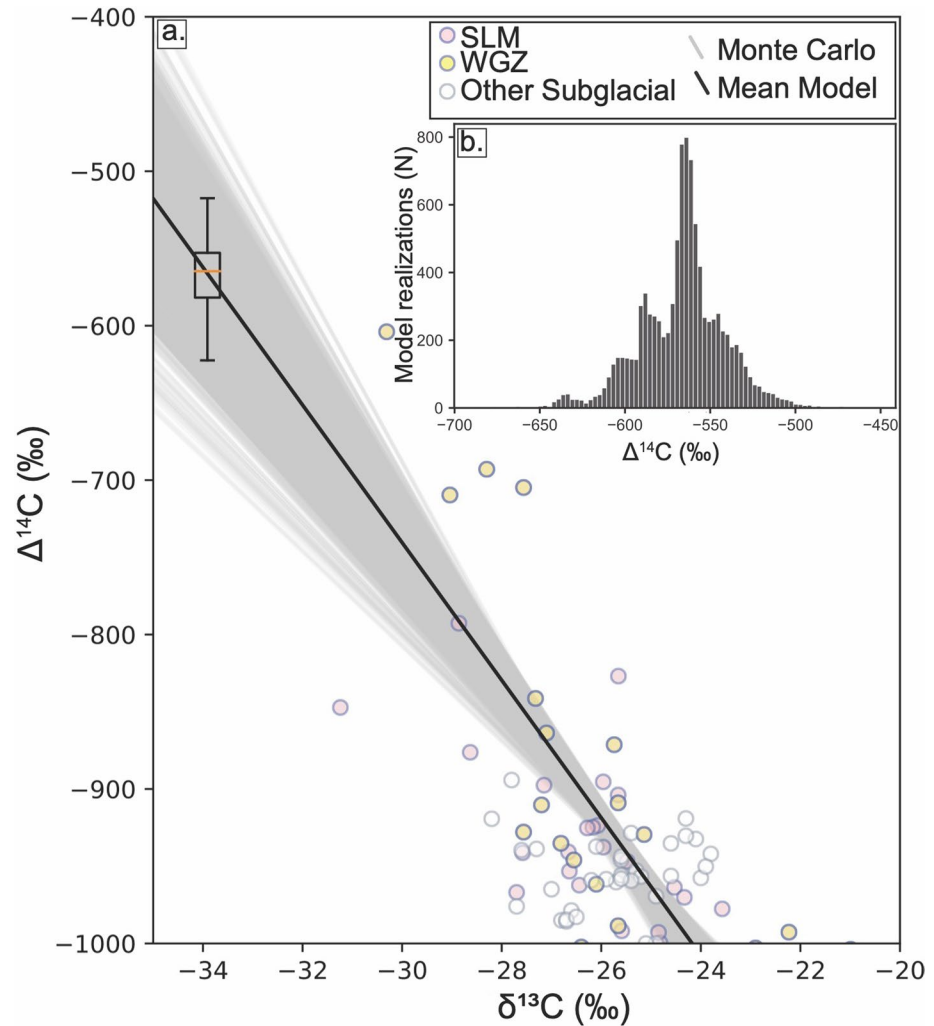
Figure 3. (a) $\delta^{13}C$ and $\Delta^{14}C$ for this study (pink) and other sediments [yellow (Venturelli et al., 2020), white (Kingslake et al., 2018)] collected from the Siple Coast sub-ice-shelf and subglacial environment. All linear models from our Monte Carlo sampling ($N = 10,000$; gray lines), as well as the mean linear model (black line) are shown. Box indicates the interquartile range of simulated $\Delta^{14}C$ values estimated at $\delta^{13}C = -33.9‰$, highlighting the mean (orange line) and 95% confidence interval (whiskers). (b) Histogram showing the distribution of $\Delta^{14}C$ values at the "new carbon" endmember ($\delta^{13}C = -33.9‰$) from our Monte Carlo simulation.

supports this assertion by determining that 79% of the total 0.715 km³ water volume in the lake was derived from basal melt of WAIS and 21% was derived from basal melt of EAIS (Text S4 in Supporting Information S1).

Using the output from our linear model ($\Delta^{14}C = -566‰$) as our estimate of "new" organic carbon in the sediment, and a ^{14}C-free input from the "old" reservoirs ($-1,000‰$), we calculated the proportion of the DIC reservoir that originated in Mercer Subglacial Lake SOC (referred to as p_{new}):

$$p_{new} = 1 - \frac{\Delta_{DIC-measured} - \Delta_{new}}{\Delta_{old} - \Delta_{new}} = 1 - \frac{-979‰ + 566‰}{-1000‰ + 566‰} = 0.049 \tag{1}$$

To determine the amount of new (^{14}C-bearing) carbon in the DIC reservoir, we multiplied p_{new} by the size of the reservoir (Table 2):

$$p_{new} \times DIC\,reservoir = 0.049 \times 7.69 \times 10^9 g\,C = 3.77 \times 10^8\,g\,^{14}C\,bearing\,DIC \tag{2}$$

We determined a mass of 10^8 g of "new" carbon translocated from SOC to DIC. We invoke heterotrophic respiration as the primary mechanism which moves carbon from the SOC to DIC pool following the findings of Achberger (2016) and Vick-Majors et al. (2016). To determine the rate at which this remineralization
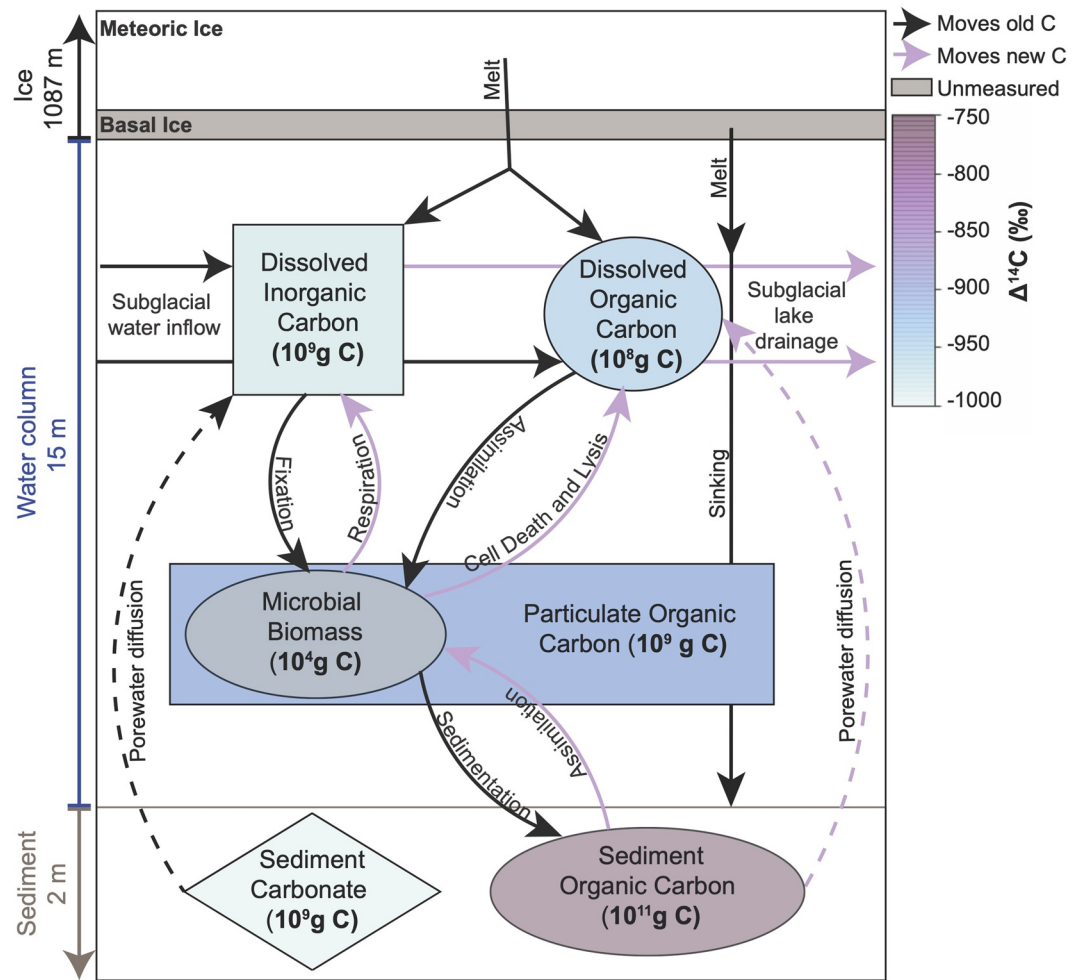
Figure 4. Conceptual model of subglacial carbon cycling in Mercer Subglacial Lake. Reservoir sizes and colors are based upon carbon content and isotopic measurements of dissolved inorganic carbon (DIC), dissolved organic carbon (DOC), particulate organic carbon (POC), sediment organic carbon (SOC), and sediment carbonate minerals. Carbon reservoirs colored gray do not have associated isotopic measurements. We mark carbon transfer between reservoirs with arrows, but note that the only biological process measured in this study was microbial respiration. Colored arrows show the inferred dominant age being moved for each process with old (>50,000 year old) carbon (black) and new (<50,000 year old) carbon (purple).

of ^{14}C-bearing SOC occurred, we divide the "new" portion of DIC by the total number of days in the 4.5-year fill-period prior to our sampling:

$$\frac{3.77 \times 10^8 \, \text{g}}{1643.625 \, \text{d}} = 2.29 \times 10^5 \, \text{g C/d} \tag{3}$$

4.2.2. The Inland Extent of Deglacial Grounding Line Retreat

We can use the rate of microbial translocation of carbon from young SOC to radiocarbon-free lake water to constrain deglacial grounding line retreat extent. Our calculated rate of carbon transfer from SOC to DIC (2.29×10^5 g C d^{-1}) is an order of magnitude higher than heterotrophic production rates (1.4×10^4 g C d^{-1}) measured directly at the sediment-water interface at the time of sampling, assuming quantitative remineralization to DIC after assimilation (i.e., a maximum estimate). The most parsimonious explanation for this order-of-magnitude difference between measured and calculated remineralization rates is that ^{14}C-bearing SOC is being remineralized from sediment-floored subglacial channels that transport water into Mercer Subglacial Lake, and the resulting ^{14}C-bearing DIC has been accumulating in the lake during the fill period prior to our sampling. In other words, the area over which remineralization is occurring extends further inland than Mercer Subglacial Lake itself.

To close the carbon budget and explain our observation, we calculated how large an area over which observed rates of remineralization would have to have been occurring as the lake filled with water during the 4.5 years prior to our sampling:

$$\left(1.4 \times 10^4 \, \mathrm{g\,C\,d^{-1}}\right) \times 1643.625 \, \mathrm{d} = 2.3 \times 10^7 \, \mathrm{g\,C} \tag{4}$$

We then divided the resulting mass by the area of Mercer Subglacial Lake to determine how much carbon is transferred from the sediment to the water column per square km.

$$\frac{2.3 \times 10^7 \, \mathrm{g\,C}}{143 \, \mathrm{km^2}} = 1.61 \times 10^5 \, \mathrm{g\,C\,km^{-2}} \tag{5}$$

Finally, we divided the mass of ^{14}C-bearing DIC from Equation 2 by the value computed in Equation 5 and removed the area of modern Mercer Subglacial Lake to find the area over which remineralization at the observed rate would have had to occur to explain our measured DIC Δ^{14}C values:

$$\frac{3.77 \times 10^8 \, \mathrm{g\,C}}{1.61 \times 10^5 \, \mathrm{g\,C\,km^{-2}}} = 2.34 \times 10^3 \, \mathrm{km^2} - 143 \, \mathrm{km^2} = 2200 \, \mathrm{km^2} \tag{6}$$

The observed remineralization occurring in Mercer Subglacial Lake therefore extended upstream from the lake over an area of 2,200 km^2 during the 4.5 years water accumulated prior to our sampling. If we assume that grounding line retreat occurred through the deepest trough in the subglacial water catchment along Mercer Ice Stream and a width of the subglacial water-flow path feeding Mercer Subglacial Lake of 20 km (Carter et al., 2013), we conclude that sediments underlying the flow path contain ^{14}C up to 110 km inland. This means that southernmost extent of deglacial grounding line retreat would have reached a total of 260 km inland from where we observe the Mercer Ice Stream grounding line today. This analysis suggests that there exists an inland limit where ^{14}C is no longer present in the subglacial sediment of AIS, and discovery of the location of this limit would delineate the portion of AIS that remained grounded throughout the last deglaciation. Such a delineation is crucial to the full calculation of ice mass loss since the LGM for assessing paleo-ice-sheet models.

Whereas past microbial activity can delineate past grounding line extent, contemporary microbial activity demonstrates the importance of a 6.3 ka marine incursion to this previously unobserved microbial ecosystem. Translocation of ^{14}C from SOC to water column DIC takes place via respiratory hydrolysis of organic matter by heterotrophic microorganisms. A significantly higher concentration of microbial biomass was present at the sediment-water interface (0–2 cm) than at depth in Mercer Subglacial Lake sediment (Davis et al., 2023). Thus, the growth and biogeochemical activities of heterotrophic bacteria and archaea in the surficial sediments provide the dominant mechanism by which organic matter oxidation transfers ^{14}C to the water column. We measured higher Δ^{14}C values in the diamict SOC compared to the lake sediment SOC, which indicates that heterotrophic microorganisms at the sediment-water interface preferentially transform ^{14}C-bearing organic matter. This preference implies that ^{14}C-bearing organic matter may be more bioavailable than the ^{14}C-free carbon pool.

5. Conclusions

We cleanly accessed a subglacial lake beneath 1,087 m of ice to sample water and sediment. Sediment organic matter allows us to constrain the most recent possible date of a marine incursion to 6.3 ± 1.0 ka. Our carbon isotopic analysis of water and sediment show that Holocene microbial activity delineates a grounding line that was substantially farther (as much as 250 km) inland than the current position of Mercer Subglacial Lake and that contemporary microbial metabolism is likely driven by assimilated marine carbon from this incursion. Our interpretations illustrate a more dynamic WAIS than previous studies (e.g., Bentley et al., 2014; Conway et al., 1999; Halberstadt et al., 2016) and outline clear subglacial targets for precise delineation of paleo grounding lines, which will yield a markedly improved understanding of ice-sheet mass changes during the Holocene.

Conflict of Interest

The authors declare no conflicts of interest relevant to this study.

Data Availability Statement

All data included in this manuscript are available at the United States Antarctic Program Data Center (USAP-DC) and can be accessed at: https://doi.org/10.15784/601672.

References

Achberger, A. M. (2016). Structure and functional potential of microbial communities in Subglacial Lake Whillans and at the Ross Ice Shelf grounding zone. https://doi.org/10.31390/gradschool_dissertations.44530

Bentley, M. J., Christoffersen, P., Hodgson, D. A., Smith, A. M., Tulaczyk, S., & Le Brocq, A. M. (2011). Subglacial lake sediments and sedimentary processes: Potential archives of ice sheet evolution, past environmental change, and the presence of life. In M. J. Siegert, M. C. Kennicutt, & R. A. Bindschadler (Eds.), *Geophysical Monograph Series* (Vol. 192, pp. 83–110). American Geophysical Union. https://doi.org/10.1029/2010GM000940

Bentley, M. J., Ó Cofaigh, C., Anderson, J. B., Conway, H., Davies, B., Graham, A. G. C., et al. (2014). A community-based geological reconstruction of Antarctic ice sheet deglaciation since the last glacial maximum. *Quaternary Science Reviews*, *100*, 1–9. https://doi.org/10.1016/j.quascirev.2014.06.025

Bindschadler, R. A., Vornberger, P. L., Stephenson, S. N., Roberts, E. P., Shabtaie, S., & MacAyeal, D. R. (1988). Ice-shelf flow at the boundary of crary ice rise, Antarctica. *Annals of Glaciology*, *11*, 8–13. https://doi.org/10.3189/S0260305500006248

Buizert, C., Cuffey, K. M., Severinghaus, J. P., Baggenstos, D., Fudge, T. J., Steig, E. J., et al. (2015). The WAIS Divide deep ice core WD2014 chronology—Part 1: Methane synchronization (68–31 ka BP) and the gas age–ice age difference. *Climate of the Past*, *11*(2), 153–173. https://doi.org/10.5194/cp-11-153-2015

Carter, S. P., & Fricker, H. A. (2012). The supply of subglacial meltwater to the grounding line of the Siple Coast, West Antarctica. *Annals of Glaciology*, *53*(60), 267–280. https://doi.org/10.3189/2012AoG60A119

Carter, S. P., Fricker, H. A., & Siegfried, M. R. (2013). Evidence of rapid subglacial water piracy under Whillans ice stream, west Antarctica. *Journal of Glaciology*, *59*(218), 1147–1162. https://doi.org/10.3189/2013JoG13J085

Chin-Leo, G., & Kirchman, D. L. (1988). Estimating bacterial production in marine waters from the simultaneous incorporation of thymidine and leucine. *Applied and Environmental Microbiology*, *54*(8), 1934–1939. https://doi.org/10.1128/aem.54.8.1934-1939.1988

Conway, H., Hall, B. L., Denton, G. H., Gades, A. M., & Waddington, E. D. (1999). Past and future grounding-line retreat of the West Antarctic ice sheet. *Science*, *286*(5438), 280–283. https://doi.org/10.1126/science.286.5438.280

Davis, C. L., Venturelli, R. A., Michaud, A. B., Hawkings, J. R., Achberger, A. M., Vick-Majors, T. J., et al. (2023). Biogeochemical and historical drivers of microbial community composition and structure in sediments from Mercer Subglacial Lake, West Antarctica. *ISME COMMUN*, *3*(1), 8. https://doi.org/10.1038/s43705-023-00216-w

DeConto, R. M., Pollard, D., Alley, R. B., Velicogna, I., Gasson, E., Gomez, N., et al. (2021). The Paris climate agreement and future sea-level rise from Antarctica. *Nature*, *593*(7857), 83–89. https://doi.org/10.1038/s41586-021-03427-0

Depoorter, M. A., Bamber, J. L., Griggs, J. A., Lenaerts, J. T. M., Ligtenberg, S. R. M., van den Broeke, M. R., & Moholdt, G. (2013). Calving fluxes and basal melt rates of Antarctic ice shelves. *Nature*, *502*(7469), 89–92. https://doi.org/10.1038/nature12567

Eglinton, T. I., Eglinton, G., Dupont, L., Sholkovitz, E. R., Montluçon, D., & Reddy, C. M. (2002). Composition, age, and provenance of organic matter in NW African dust over the Atlantic Ocean. *Geochemistry, Geophysics, Geosystems*, *3*(8), 1–27. https://doi.org/10.1029/2001GC000269

Engelhardt, H., & Kamb, B. (1997). Basal hydraulic system of a West Antarctic ice stream: Constraints from borehole observations. *Journal of Glaciology*, *43*(144), 207–230. https://doi.org/10.3189/S0022143000003166

Fernandez, A., Santos, G. M., Williams, E. K., Pendergraft, M. A., Vetter, L., & Rosenheim, B. E. (2014). Blank corrections for ramped pyrolysis radiocarbon dating of sedimentary and soil organic carbon. *Analytical Chemistry*, *86*(24), 12085–12092. https://doi.org/10.1021/ac502874j

French, S. A., Clark, M. R., Smith, R. J., Brind, T., & Hawkins, B. C. (2018). Expedient synthesis of xanthones and multi-functionalized chromones from 1,1-diacyl cyclopropanes. *Tetrahedron*, *74*(38), 5340–5350. https://doi.org/10.1016/j.tet.2018.04.003

Greenwood, S. L., Simkins, L. M., Halberstadt, A. R. W., Prothro, L. O., & Anderson, J. B. (2018). Holocene reconfiguration and readvance of the East Antarctic Ice Sheet. *Nature Communications*, *9*(1), 3176. https://doi.org/10.1038/s41467-018-05625-3

Gough, M. A., Fauzi, R., Mantoura, C., & Preston, M. (1993). Terrestrial plant biopolymers in marine sediments. *Geochimica et Cosmochimica Acta*, *57*(5), 945–964. https://doi.org/10.1016/0016-7037(93)90032-R

Gustafson, C. D., Key, K., Siegfried, M. R., Winberry, J. P., Fricker, H. A., Venturelli, R. A., & Michaud, A. B. (2022). A dynamic saline groundwater system mapped beneath an Antarctic ice stream. *Science*, *376*(6593), 640–644. https://doi.org/10.1126/science.abm3301

Halberstadt, A. R. W., Simkins, L. M., Greenwood, S. L., & Anderson, J. B. (2016). Past ice-sheet behaviour: Retreat scenarios and changing controls in the Ross Sea, Antarctica. *The Cryosphere*, *10*(3), 1003–1020. https://doi.org/10.5194/tc-10-1003-2016

Heaton, T. J., Köhler, P., Butzin, M., Bard, E., Reimer, R. W., Austin, W. E. N., et al. (2020). Marine20—The marine radiocarbon age calibration curve (0–55,000 cal BP). *Radiocarbon*, *62*(4), 779–820. https://doi.org/10.1017/RDC.2020.68

Hernes, P. J., & Benner, R. (2006). Terrigenous organic matter sources and reactivity in the North Atlantic Ocean and a comparison to the Arctic and Pacific oceans. *Marine Chemistry*, *100*(1), 66–79. https://doi.org/10.1016/j.marchem.2005.11.003

Hernes, P. J., Robinson, A. C., & Aufdenkampe, A. K. (2007). Fractionation of lignin during leaching and sorption and implications for organic matter "freshness". *Geophysical Research Letters*, *34*(17), L17401. https://doi.org/10.1029/2007GL031017

Hopmans, E. C., Schouten, S., & Sinninghe Damsté, J. S. (2016). The effect of improved chromatography on GDGT-based palaeoproxies. *Organic Geochemistry*, *93*, 1–6. https://doi.org/10.1016/j.orggeochem.2015.12.006

Horrigan, S. G. (1981). Primary production under the Ross ice shelf, Antarctica1. *Limnology & Oceanography*, *26*(2), 378–382. https://doi.org/10.4319/lo.1981.26.2.0378

Johnson, J. S., Venturelli, R. A., Balco, G., Allen, C. S., Braddock, S., Campbell, S., et al. (2022). Review article: Existing and potential evidence for Holocene grounding line retreat and readvance in Antarctica. *The Cryosphere*, *16*(5), 1543–1562. https://doi.org/10.5194/tc-16-1543-2022

Jones, R. S., Johnson, J. S., Lin, Y., Mackintosh, A. N., Sefton, J. P., Smith, J. A., et al. (2022). Stability of the Antarctic ice sheet during the pre-industrial Holocene. *Nature Reviews Earth & Environment*, *3*(8), 500–515. https://doi.org/10.1038/s43017-022-00309-5

Kamb, B. (2001). Basal Zone of the West Antarctic ice streams and its role in lubrication of their rapid motion. In R. B. Alley & R. A. Bindschadle (Eds.), *Antarctic research series* (pp. 157–199). American Geophysical Union. https://doi.org/10.1029/AR077p0157

Kepner, R. L., Wharton, R. A., & Suttle, C. A. (1998). Viruses in Antarctic lakes. *Limnology & Oceanography*, *43*(7), 1754–1761. https://doi.org/10.4319/lo.1998.43.7.1754

King, M. A., Watson, C. S., & White, D. (2022). GPS rates of vertical bedrock motion suggest Late Holocene ice-sheet readvance in a critical sector of East Antarctica. *Geophysical Research Letters*, *49*(4), e2021GL097232. https://doi.org/10.1029/2021GL097232

Kingslake, J., Scherer, R. P., Albrecht, T., Coenen, J., Powell, R. D., Reese, R., et al. (2018). Extensive retreat and re-advance of the West Antarctic ice sheet during the Holocene. *Nature*, *558*(7710), 430–434. https://doi.org/10.1038/s41586-018-0208-x

Kopp, R. E., Kemp, A. C., Bittermann, K., Horton, B. P., Donnelly, J. P., Gehrels, W. R., et al. (2016). Temperature-driven global sea-level variability in the Common Era. *Proceedings of the National Academy of Sciences of the United States of America*, *113*(11). https://doi.org/10.1073/pnas.1517056113

Libby, W. F. (1955). *Radiocarbon dating* (Vol. 37). University of Chicago Press.

Livingstone, S. J., Li, Y., Rutishauser, A., Sanderson, R. J., Winter, K., Mikucki, J. A., et al. (2022). Subglacial lakes and their changing role in a warming climate. *Nature Reviews Earth & Environment*, *3*(2), 106–124. https://doi.org/10.1038/s43017-021-00246-9

McNichol, A. P., Jones, G. A., Hutton, D. L., Gagnon, A. R., & Key, R. M. (1994). The rapid preparation of seawater ΣCO2 for radiocarbon analysis at the National Ocean Sciences Ams Facility. *Radiocarbon*, *36*(2), 237–246. https://doi.org/10.1017/S0033822200040522

Meredith, M., Sommerkorn, M., Cassotta, S., Derksen, C., Ekaykin, A., Hollowed, A., et al. (2019). Polar Regions. In H.-O. Pörtner, D. C. Roberts, V. Masson-Delmotte, P. Zhai, M. Tignor, E. Poloczanska (Eds.), *IPCC Special Report on the Ocean and Cryosphere in a Changing Climate* (pp. 203–320). Cambridge University Press, Cambridge, UK and New York, NY, USA. https://doi.org/10.1017/9781009157964.005

Mercer, J. H. (1978). West Antarctic ice sheet and CO_2 greenhouse effect: A threat of disaster. *Nature*, *271*, 321–325. https://doi.org/10.1038/271321a0

Michaud, A. B., Vick-Majors, T. J., Achberger, A. M., Skidmore, M. L., Christner, B. C., Tranter, M., & Priscu, J. C. (2020). Environmentally clean access to Antarctic subglacial aquatic environments. *Antarctic Science*, *32*(5), 329–340. https://doi.org/10.1017/S0954102020000231

Monson, K. D., & Hayes, J. M. (1982). Carbon isotopic fractionation in the biosynthesis of bacterial fatty acids. Ozonolysis of unsaturated fatty acids as a means of determining the intramolecular distribution of carbon isotopes. *Geochimica et Cosmochimica Acta*, *46*(2), 139–149. https://doi.org/10.1016/0016-7037(82)90241-1

Mouginot, J., Rignot, E., & Scheuchl, B. (2019). Continent-wide, interferometric SAR phase, mapping of Antarctic ice velocity. *Geophysical Research Letters*, *46*(16), 9710–9718. https://doi.org/10.1029/2019GL083826

National Research Council. (2007). *Exploration of Antarctic subglacial aquatic environments: Environmental and scientific stewardship*. The National Academies Press. https://doi.org/10.17226/11886

Neuhaus, S. U., Tulaczyk, S. M., Stansell, N. D., Coenen, J. J., Scherer, R. P., Mikucki, J. A., & Powell, R. D. (2021). Did Holocene climate changes drive West Antarctic grounding line retreat and readvance? *The Cryosphere*, *15*(10), 4655–4673. https://doi.org/10.5194/tc-15-4655-2021

Nicholls, R. J., Hanson, S. E., Lowe, J. A., Slangen, A. B. A., Wahl, T., Hinkel, J., & Long, A. J. (2021). Integrating new sea-level scenarios into coastal risk and adaptation assessments: An ongoing process. *WIREs Climate Change*, *12*(3), e706. https://doi.org/10.1002/wcc.706

Priscu, J. C., Achberger, A. M., Cahoon, J. E., Christner, B. C., Edwards, R. L., Jones, W. L., et al. (2013). A microbiologically clean strategy for access to the Whillans Ice Stream subglacial environment. *Antarctic Science*, *25*(5), 637–647. https://doi.org/10.1017/S0954102013000035

Priscu, J. C., Downes, M. T., Priscu, L. R., Palmisano, A. C., & Sullivan, C. W. (1990). Dynamics of ammonium oxidizer activity and nitrous oxide (N₂O) within and beneath Antarctic sea ice (p. 11).

Priscu, J. C., Kalin, J., Winans, J., Campbell, T., Siegfried, M. R., Skidmore, M., et al. (2021). Scientific access into Mercer Subglacial Lake: Scientific objectives, drilling operations and initial observations. *Annals of Glaciology*, *62*(85–86), 340–352. https://doi.org/10.1017/aog.2021.10

Prothro, L. O., Majewski, W., Yokoyama, Y., Simkins, L. M., Anderson, J. B., Yamane, M., et al. (2020). Timing and pathways of East Antarctic ice sheet retreat. *Quaternary Science Reviews*, *230*, 106166. https://doi.org/10.1016/j.quascirev.2020.106166

Prothro, L. O., Simkins, L. M., Majewski, W., & Anderson, J. B. (2018). Glacial retreat patterns and processes determined from integrated sedimentology and geomorphology records. *Marine Geology*, *395*, 104–119. https://doi.org/10.1016/j.margeo.2017.09.012

Rack, F. R. (2016). Enabling clean access into Subglacial Lake Whillans: Development and use of the WISSARD hot water drill system. *Philosophical Transactions of the Royal Society A: Mathematical, Physical & Engineering Sciences*, *374*(2059), 20140305. https://doi.org/10.1098/rsta.2014.0305

Rignot, E., Mouginot, J., Scheuchl, B., Broeke, M., Wessem, M. J., & Morlighem, M. (2019). Four decades of Antarctic Ice Sheet mass balance from 1979–2017. *Proceedings of the National Academy of Sciences*, *116*(4), 1095–1103. https://doi.org/10.1073/pnas.1812883116

Robel, A. A., Seroussi, H., & Roe, G. H. (2019). Marine ice sheet instability amplifies and skews uncertainty in projections of future sea-level rise. *Proceedings of the National Academy of Sciences*, *116*(30), 14887–14892. https://doi.org/10.1073/pnas.1904822116

Rosenheim, B. E., Day, M. B., Domack, E., Schrum, H., Benthien, A., & Hayes, J. M. (2008). Antarctic sediment chronology by programmed-temperature pyrolysis: Methodology and data treatment: Pyrolysis of Antarctic sediments. *Geochemistry, Geophysics, Geosystems*, *9*(4), Q04005. https://doi.org/10.1029/2007GC001816

Rosenheim, B. E., Michaud, A. B., Broda, J., Gagnon, A., Venturelli, R. A., Campbell, T., et al. (2023). A method for successful collection of multicores and gravity cores from Antarctic subglacial lakes. *Limnology and Oceanography: Methods*. https://doi.org/10.1002/lom3.10545

Rosenheim, B. E., Santoro, J. A., Gunter, M., & Domack, E. W. (2013). Improving Antarctic sediment 14C dating using ramped pyrolysis: An example from the Hugo Island Trough. *Radiocarbon*, *55*(1), 115–126. https://doi.org/10.2458/azu_js_rc.v55i1.16234

Scambos, T. A., Haran, T. M., Fahnestock, M. A., Painter, T. H., & Bohlander, J. (2007). MODIS-based Mosaic of Antarctica (MOA) data sets: Continent-wide surface morphology and snow grain size. *Remote Sensing of Environment*, *111*(2), 242–257. https://doi.org/10.1016/j.rse.2006.12.020

Schoof, C. (2007). Marine ice-sheet dynamics. Part 1. The case of rapid sliding. *Journal of Fluid Mechanics*, *573*, 27–55. https://doi.org/10.1017/S0022112006003570

Sessions, A. (2006). Isotope-ratio detection for gas chromatography. *Journal of Separation Science*, *29*(12), 1946–1961. https://doi.org/10.1002/jssc.200600002

Siegfried, M. R., & Fricker, H. A. (2018). Thirteen years of subglacial lake activity in Antarctica from multi-mission satellite altimetry. *Annals of Glaciology*, *59*(76pt1), 42–55. https://doi.org/10.1017/aog.2017.36

Siegfried, M. R., & Fricker, H. A. (2021). Illuminating active Subglacial Lake processes with ICESat-2 laser altimetry. *Geophysical Research Letters*, *48*(14), e2020GL091089. https://doi.org/10.1029/2020GL091089

Siegfried, M. R., Fricker, H. A., Carter, S. P., & Tulaczyk, S. (2016). Episodic ice velocity fluctuations triggered by a subglacial flood in West Antarctica. *Geophysical Research Letters*, *43*(6), 2640–2648. https://doi.org/10.1002/2016GL067758

Siegfried, M. R., Venturelli, R. A., Patterson, M. O., Arnuk, W., Campbell, T. D., Gustafson, C. D., et al. (2023). The life and death of a subglacial lake in West Antarctica. *Geology*. https://doi.org/10.1130/G50995.1

Smith, B., Fricker, H. A., Gardner, A. S., Medley, B., Nilsson, J., Paolo, F. S., et al. (2020). Pervasive ice sheet mass loss reflects competing ocean and atmosphere processes. *Science*, *368*(6496), 1239–1242. https://doi.org/10.1126/science.aaz5845

Stone, J. O., Balco, G. A., Sugden, D. E., Caffee, M. W., Sass, L. C., Cowdery, S. G., & Siddoway, C. (2003). Holocene deglaciation of Marie Byrd land, west Antarctica. *Science*, *299*(5603), 99–102. https://doi.org/10.1126/science.1077998

Subt, C., Yoon, H. I., Yoo, K. C., Lee, J. I., Leventer, A., Domack, E. W., & Rosenheim, B. E. (2017). Sub-ice shelf sediment geochronology utilizing novel radiocarbon methodology for highly detrital sediments: Chronology for highly detrital sediments. *Geochemistry, Geophysics, Geosystems*, *18*(4), 1404–1418. https://doi.org/10.1002/2016GC006578

Sun, S., Schefuß, E., Mulitza, S., Chiessi, C. M., Sawakuchi, A. O., Zabel, M., et al. (2017). Origin and processing of terrestrial organic carbon in the Amazon system: Lignin phenols in river, shelf, and fan sediments. *Biogeosciences*, *14*(9), 2495–2512. https://doi.org/10.5194/bg-14-2495-2017

Tulaczyk, S., Mikucki, J. A., Siegfried, M. R., Priscu, J. C., Barcheck, C. G., Beem, L. H., et al. (2014). WISSARD at Subglacial Lake Whillans, West Antarctica: Scientific operations and initial observations. *Annals of Glaciology*, *55*(65), 51–58. https://doi.org/10.3189/2014AoG65A009

Venturelli, R. A., Ryan, A., Vick-Majors, T. J., Collins, B., Gagnon, A., Kasic, K., et al. (2021). A framework for trandisciplinary radiocarbon research: Use of natural-level and elevated-level ^{14}C in Antarctic field research. *Radiocarbon*, *63*(5), 1–14. https://doi.org/10.1017/RDC.2021.55

Venturelli, R. A., Siegfried, M. R., Roush, K. A., Li, W., Burnett, J., Zook, R., et al. (2020). Mid-Holocene grounding line retreat and readvance at Whillans ice stream, west Antarctica. *Geophysical Research Letters*, *47*(15), e2020GL088476. https://doi.org/10.1029/2020GL088476

Vick-Majors, T. J., Achberger, A., Santibáñez, P., Dore, J. E., Hodson, T., Michaud, A. B., et al. (2016). Biogeochemistry and microbial diversity in the marine cavity beneath the McMurdo Ice Shelf, Antarctica: Biogeochemistry under the MCM ice shelf. *Limnology & Oceanography*, *61*(2), 572–586. https://doi.org/10.1002/lno.10234

Villinski, J. C., Dunbar, R. B., & Mucciarone, D. A. (2000). Carbon 13/carbon 12 ratios of sedimentary organic matter from the Ross Sea, Antarctica: A record of phytoplankton bloom dynamics. *Journal of Geophysical Research*, *105*(C6), 14163–14172. https://doi.org/10.1029/1999JC000309

Walker, B. D., & Xu, X. (2019). An improved method for the sealed-tube zinc graphitization of microgram carbon samples and ^{14}C AMS measurement. *Nuclear Instruments and Methods in Physics Research Section B: Beam Interactions with Materials and Atoms*, *438*, 58–65. https://doi.org/10.1016/j.nimb.2018.08.004

Weertman, J. (1974). Stability of the junction of an ice sheet and an ice shelf. *Journal of Glaciology*, *13*(67), 3–11. https://doi.org/10.3189/S0022143000023327

Wessel, P., Luis, J. F., Uieda, L., Scharroo, R., Wobbe, F., Smith, W. H. F., & Tian, D. (2019). The generic mapping tools version 6. *Geochemistry, Geophysics, Geosystems*, *20*(11), 5556–5564. https://doi.org/10.1029/2019GC008515

Xu, L., Roberts, M. L., Elder, K. L., Kurz, M. D., McNichol, A. P., Reddy, C. M., et al. (2021). Radiocarbon in dissolved organic carbon by UV oxidation: Procedures and blank characterization at NOSAMS. *Radiocarbon*, *61*(1), 357–374. https://doi.org/10.1017/rdc.2020.102

Yan, S., Blankenship, D. D., Greenbaum, J. S., Young, D. A., Li, L., Rutishauser, A., et al. (2022). A newly discovered subglacial lake in East Antarctica likely hosts a valuable sedimentary record of ice and climate change. *Geology*, *50*(8), 949–953. https://doi.org/10.1130/G50009.1

References From the Supporting Information

Alley, K. E., Scambos, T. A., Siegfried, M. R., & Fricker, H. A. (2016). Impacts of warm water on Antarctic ice shelf stability through basal channel formation. *Nature Geoscience*, *9*(4), 290–293. https://doi.org/10.1038/ngeo2675

Barrett, P. J., Elliot, D. H., & Lindsay, J. F. (1986). The Beacon supergroup (Devonian-Triassic) and Ferrar group (Jurrasic) in the Beardmore Glacier area, Antarctica. In *Antarctic research series*. https://doi.org/10.1029/AR036p0339

Brown, C. A. (1960). Palynological techniques (p. 226). Retrieved from https://digitalcommons.usu.edu/bee_lab_bo/226

Coenen, J. J., Scherer, R. P., Baudoin, P., Warny, S., Castañeda, I. S., & Askin, R. (2020). Paleogene marine and terrestrial development of the West Antarctic rift system. *Geophysical Research Letters*, *47*(3), e2019GL085281. https://doi.org/10.1029/2019GL085281

Erskine, R. H., Green, T. R., Ramirez, J. A., & MacDonald, L. H. (2006). Comparison of grid-based algorithms for computing upslope contributing area. *Water Resources Research*, *42*(9). https://doi.org/10.1029/2005WR004648

Feakins, S. J., Warny, S., & Lee, J.-E. (2012). Hydrologic cycling over Antarctica during the middle Miocene warming. *Nature Geoscience*, *5*(8), 557–560. https://doi.org/10.1038/ngeo1498

Fricker, H. A., & Scambos, T. A. (2009). Connected subglacial lake activity on lower mercer and Whillans ice streams, West Antarctica, 2003–2008. *Journal of Glaciology*, *55*(190), 303–315. https://doi.org/10.3189/002214309788608813

Hannah, M. J., Wilson, G. J., & Wrenn, J. H. (2000). Oligocene and Miocene marine palynomorphs from CRP-2/2A, Victoria land basin, Antarctica. *Terra Antartica*, *7*(4), 503–511.

Harwood, D. M., & Bohaty, S. M. (2001). Early Oligocene Siliceous Microfossil Biostratigraphy of Cape Roberts Project Core CRP-3, Victoria Land Basin, Antarctica. *Terra Antartica*, *8*(4), 315–338.

Harwood, D. M., Scherer, R. P., & Webb, P.-N. (1989). Multiple Miocene marine productivity events in West Antarctica as recorded in upper Miocene sediments beneath the Ross ice shelf (site J-9). *Marine Micropaleontology*, *15*(1), 91–115. https://doi.org/10.1016/0377-8398(89)90006-6

Hedges, J. I., & Ertel, J. R. (1982). Characterization of lignin by gas capillary chromatography of cupric oxide oxidation products. *Analytical Chemistry*, *54*(2), 174–178. https://doi.org/10.1021/ac00239a007

Jex, C. N., Pate, G. H., Blyth, A. J., Spencer, R. G. M., Hernes, P. J., Khan, S. J., & Baker, A. (2014). Lignin biogeochemistry: From modern processes to quaternary archives. *Quaternary Science Reviews*, *87*, 46–59. https://doi.org/10.1016/j.quascirev.2013.12.028

Joughin, I., Tulaczyk, S., MacAyeal, D. R., & Engelhardt, H. (2004). Melting and freezing beneath the Ross ice streams, Antarctica. *Journal of Glaciology*, *50*(168), 96–108. https://doi.org/10.3189/172756504781830295

Le Brocq, A. M., Payne, A. J., Siegert, M. J., & Alley, R. B. (2009). A subglacial water-flow model for West Antarctica. *Journal of Glaciology*, *55*(193), 879–888. https://doi.org/10.3189/002214309790152564

Le Brocq, A. M., Anne, M., Ross, N., Griggs, J. A., Bingham, R. G., Corr, H. F. J., et al. (2013). Evidence from ice shelves for channelized meltwater flow beneath the Antarctic Ice Sheet. *Nature Geoscience*, *6*(11), 945–948. https://doi.org/10.1038/ngeo1977

Morlighem, M., Rignot, E., Binder, T., Blankenship, D., Drews, R., Eagles, G., et al. (2020). Deep glacial troughs and stabilizing ridges unveiled beneath the margins of the Antarctic ice sheet. *Nature Geoscience*, *13*(2), 132–137. https://doi.org/10.1038/s41561-019-0510-8

Mudie, P. J. (1992). Circum-Arctic quaternary and Neogene marine palynofloras: Paleoecology and statistical analysis. In *Neogene and Quaternary dinoflagellate cysts and acritarchs*.

Post, A., Hemer, M., O'Brien, P., Roberts, D., & Craven, M. (2007). History of benthic colonisation beneath the Amery ice shelf, East Antarctica. *Marine Ecology Progress Series*, *344*, 29–37. https://doi.org/10.3354/meps06966

Raine, J. I., & Askin, R. A. (2001). Terrestrial palynology of cape Roberts project Drillhole CRP-3, Victoria land basin, Antarctica. *Terra Antarctica*, *8*(4), 389–400.

Rebesco, M., Domack, E., Zgur, F., Lavoie, C., Leventer, A., Brachfeld, S., et al. (2014). Boundary condition of grounding lines prior to collapse, Larsen-B Ice Shelf, Antarctica. *Science*, *345*(6202), 1354–1358. https://doi.org/10.1126/science.1256697

Scherer, R. P. (1991). Quaternary and tertiary microfossils from beneath ice stream B: Evidence for a dynamic West Antarctic ice sheet history. *Global and Planetary Change*, *4*(4), 395–412. https://doi.org/10.1016/0921-8181(91)90005-H

Scherer, R., Bohaty, S. M., & Harwood, D. M. (2000). *Oligocene and Lower Miocene Siliceous Microfossil Biostratigraphy of Cape Roberts Project Core CRP-2/2A, Victoria Land Basin, Antarctica*. Terra Antarctica. Retrieved from https://digitalcommons.unl.edu/cgi/viewcontent.cgi?article=1285&context=geosciencefacpub

Sjunneskog, C., & Taylor, F. (2002). Postglacial marine diatom record of the Palmer deep, Antarctic Peninsula (ODP leg 178, site 1098) 1. Total diatom abundance. *Paleoceanography*, *17*(3), PAL4-1–PAL4-8. https://doi.org/10.1029/2000PA000563

Smith, J. A., Graham, A. G. C., Post, A. L., Hillenbrand, C.-D., Bart, P. J., & Powell, R. D. (2019). The marine geological imprint of Antarctic ice shelves. *Nature Communications*, *10*(1), 5635. https://doi.org/10.1038/s41467-019-13496-5

Spencer, R. G. M., Aiken, G. R., Dyda, R. Y., Butler, K. D., Bergamaschi, B., & Hernes, P. J. (2010). Comparison of XAD with other dissolved lignin isolation techniques and a compilation of analytical improvements for the analysis of lignin in aquatic settings. *Organic Geochemistry*, *41*(5), 445–453. https://doi.org/10.1016/j.orggeochem.2010.02.004

Tibbett, E. J., Scher, H. D., Warny, S., Tierney, J. E., Passchier, S., & Feakins, S. J. (2021). Late Eocene record of hydrology and temperature from Prydz Bay, East Antarctica. *Paleoceanography and Paleoclimatology*, *36*(4), e2020PA004204. https://doi.org/10.1029/2020PA004204

Van Liefferinge, B., & Pattyn, F. (2013). Using ice-flow models to evaluate potential sites of million year-old ice in Antarctica. *Climate of the Past*, *9*(5), 2335–2345. https://doi.org/10.5194/cp-9-2335-2013

Warnock, J. P., & Scherer, R. P. (2015). A revised method for determining the absolute abundance of diatoms. *Journal of Paleolimnology*, *53*(1), 157–163. https://doi.org/10.1007/s10933-014-9808-0

Warny, S., Askin, R. A., Hannah, M. J., Mohr, B. A. R., Raine, J. I., Harwood, D. M., & Florindo, F. (2009). Palynomorphs from a sediment core reveal a sudden remarkably warm Antarctica during the middle Miocene. *Geology*, *37*(10), 955–958. https://doi.org/10.1130/G30139A.1

Willis, I. C., Pope, E. L., Leysinger Vieli, G. J.-M. C., Arnold, N. S., & Long, S. (2016). Drainage networks, lakes and water fluxes beneath the Antarctic ice sheet. *Annals of Glaciology*, *57*(72), 96–108. https://doi.org/10.1017/aog.2016.15

Wrenn, J. H., Hannah, M. J., & Raine, J. I. (1998). Diversity and Palaeoenvironmental significance of late Cainozoic marine palynomorphs from the CRP-l core, Ross Sea, Antarctica. *Terra Antarctica*, *5*(3), 553–570.